

Soft Matter

Accepted Manuscript



This is an *Accepted Manuscript*, which has been through the Royal Society of Chemistry peer review process and has been accepted for publication.

Accepted Manuscripts are published online shortly after acceptance, before technical editing, formatting and proof reading. Using this free service, authors can make their results available to the community, in citable form, before we publish the edited article. We will replace this *Accepted Manuscript* with the edited and formatted *Advance Article* as soon as it is available.

You can find more information about *Accepted Manuscripts* in the [Information for Authors](#).

Please note that technical editing may introduce minor changes to the text and/or graphics, which may alter content. The journal's standard [Terms & Conditions](#) and the [Ethical guidelines](#) still apply. In no event shall the Royal Society of Chemistry be held responsible for any errors or omissions in this *Accepted Manuscript* or any consequences arising from the use of any information it contains.

Tough dual nanocomposite hydrogels with inorganic hybrid crosslinking

Received 00th January 20xx,
Accepted 00th January 20xx

Juan Du, Shimei Xu*, Shun Feng, Lina Yu, Jide Wang*, and Yumei Liu

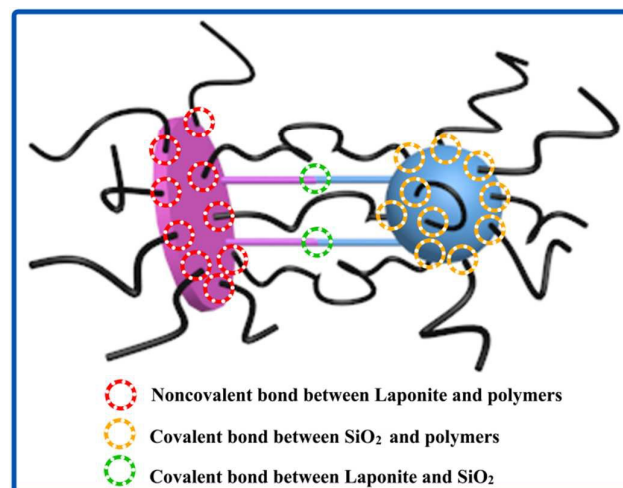
DOI: 10.1039/x0xx00000x

www.rsc.org/

A dual nanocomposite hydrogel with inorganic hybrid crosslinking was fabricated through simultaneous sol-gel technique and free radical polymerization. Due to the multi-strengthening mechanism of dual nanocomposite, the hydrogel was super tough and strong with a compressive stress of 32.00 MPa without rupture even at 100% strain, while it exhibited excellent fatigue resistant properties.

Recent progress in developing tough hydrogels promises the great potential of this class of soft and wet materials as biomaterials, soft robotics, smart actuators and sensors.¹⁻¹¹ However, the applications of hydrogels made from either natural or synthetic sources are strongly limited by poor mechanical properties due to their inhomogeneous network structure and monotonous toughening mechanism. In recent years, various types of hydrogels with enhanced mechanical properties have been developed: such as slide-ring hydrogels,¹² double network hydrogels,¹³ macromolecular microsphere composite hydrogels,¹⁴ tetra-PEG hydrogels,¹⁵ hydrophobic modified hydrogels,¹⁶ ionically cross-linked hydrogels,¹⁷ dipole-dipole and hydrogen bonding reinforced hydrogels¹⁸ and nanocomposite hydrogels.¹⁹⁻²⁶ The general principle for the design of tough hydrogels is to implement mechanisms for dissipating mechanical energy and maintaining high elasticity.^{27, 28} If either of the mechanisms becomes invalid under applied force, the hydrogel will lose its high toughness.²⁷ Combination of chain fracture/reversible crosslinking was widely used on the design of tough hydrogels. However, tough hydrogels relying on the chain-fracture mechanism will be susceptible to fatigue under multiple cycles

of large deformation while the hydrogels only using reversible crosslinking mechanism will deform plastically under loads. Thus it is still challenging for existing hydrogels to achieve comprehensive mechanical performance of some biomaterials (such as artificial cartilage, vessels, and prosthetic joints).^{27, 29, 30}



Scheme 1 Schematic representation of the structural model for the dual nanocomposite hydrogels.

Different from conventional chemical or physical crosslinking caused by organic crosslinker or Laponite in the existing hydrogels, here, we reported a dual nanocomposite hydrogel in which covalently bonded Laponite and SiO₂ were used as a multifunctional hybrid crosslinker. The exfoliated nano-Laponite was used to crosslink polymers through hydrogen bonds and coordinate bonds.¹⁹ The nano-scaled SiO₂ was embedded into the polymer matrix by covalent bonds (Scheme 1). As a result, there existed inorganic hybrid crosslinking in the dual nanocomposite hydrogel which could withstand a compressive stress of 32.00 MPa without rupture even at 100% strain and also exhibited excellent fatigue resistant properties upon five cycles. The toughness-

Key Laboratory of Oil and Gas Fine Chemicals, Ministry of Education and Xinjiang Uyghur Autonomous Region, College of Chemistry and Chemical Engineering, Xinjiang University, Urumqi, Xinjiang 830046, People's Republic of China; Fax: + 86 991 8581018; Tel: + 86 991 8583972; E-mail: xushmei@hotmail.com, awangjd@xju.edu.cn

† Electronic Supplementary Information (ESI) available: Experimental procedures; Retention time dependence of transparency and viscosity; TEM images of poly(AAm-co-MAA)/SiO₂ nanocomposite hydrogel; TEM images of poly(AAm-co-MAA)/Laponite/SiO₂ dual nanocomposite hydrogel treated by NaOH. See DOI: 10.1039/x0xx00000x

enhancement mechanism was not just the integration of polymer chain fracture/high-functionality crosslinker Laponite and silica plus meso-/macro-scale composites. More importantly, Laponite nanosheets and SiO₂ nanoparticles were connected by covalent bonds to enhance compatibility among hydrogel components and form hierarchical structure which could well maintain high elasticity under deformation.

Our design rationale for dual nanocomposite hydrogel is to utilize silica and Laponite XLG ([Mg_{5.34}Li_{0.66}Si₈O₂₀(OH)₄]Na_{0.66}) as multifunctional cross-linking agents for building a unique organic/inorganic three-dimensional network structure. In this study, γ -methacryloxypropyltrimethoxysilane (MPTMS) worked as silica source in presence of methacrylic acid (MAA) catalyst and uniform silica nanoparticles were obtained by a universal

sol-gel method.³¹ Fig. 1 showed the schematic illustration of the preparation process and structural model of the dual nanocomposite hydrogel. Laponite dispersion was first prepared as described in our previous work (Fig. 1a).³² Then acrylamide (AAm) (Fig. 1b), MPTMS (mixed with MAA beforehand), and KPS were introduced into the Laponite dispersion (Fig. 1c). There existed obvious interactions between Laponite and monomers, but the dispersion remained stable without precipitation (Fig. S1, ESI†). The dual nanocomposite hydrogels poly(AAm-co-MAA)/Laponite/SiO₂ were finally prepared by simultaneous in-situ polymerization and sol-gel process (Fig. 1d, e). And the schematic representation of multi-monomer polymerization was demonstrated in scheme 2.

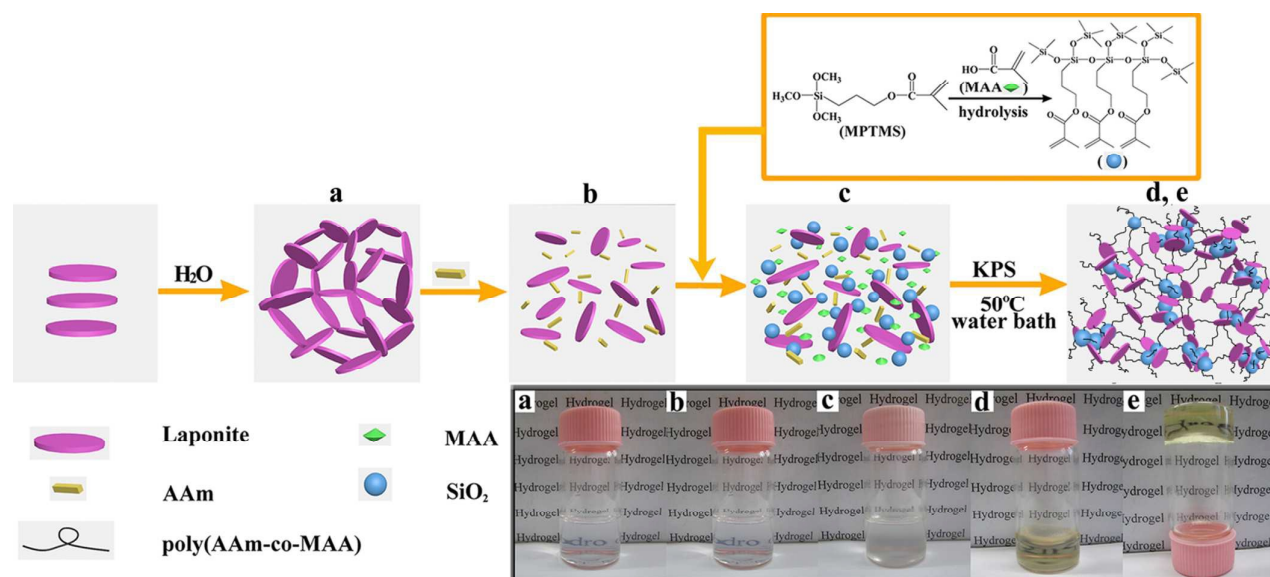
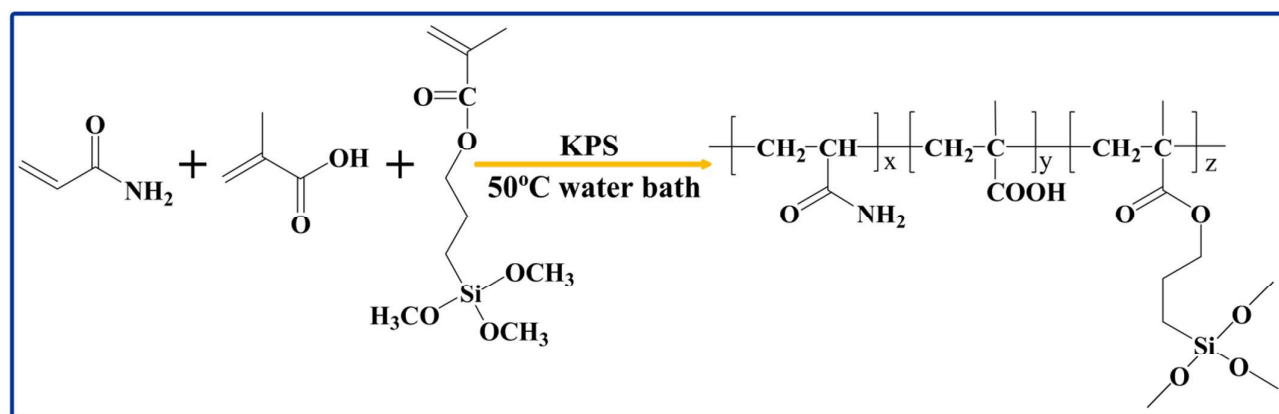


Fig. 1 Schematic preparation of poly(AAm-co-MAA)/Laponite/SiO₂ dual nanocomposite hydrogels (the insert: a-Optical images of 2 wt% of aqueous Laponite dispersion; b-Laponite mixed with AAm; c-Laponite mixed with AAm, MAA, and MPTMS; d, e-As-prepared dual nanocomposite hydrogel).



Scheme 2 Schematic representation of the multi-monomer polymerization.

Table 1 The compressive properties of the hydrogels with different cross-linking networks.

Hydrogel	Fracture strain (%)	Fracture stress (MPa)	Elastic modulus (MPa)	Toughness (MJ m^{-3})
Poly(AAm-co-MAA)/Laponite/SiO ₂	-	-	1.50	5.46 (100% strain)
Poly(AAm-co-MAA)/Laponite	79.37	11.91	0.96	1.76
Poly(AAm-co-MAA)/SiO ₂	-	-	3.5	10.74 (100% strain)
Poly(AAm-co-MAA)	92.42	2.66	0.2	0.67

The obtained dual nanocomposite hydrogels were highly rigid and durable when compressed. This hydrogel could sustain a compressive pressure as high as dozens of megapascals without any damage at a strain of 100% (Fig. 2I). The residual deformation was 1.90%, showing that this gel material had a strong deformation resistance. Moreover, this hydrogel was surprisingly resistant to slicing with a knife (Fig. 2II).

Compressive mechanical properties were investigated among the hydrogels (7 mm diameter \times 10 mm length) with different crosslinking networks to test the toughening mechanism of dual nanocomposite structure (Fig. 2III and Table 1). Nano-clay crosslinked poly(AAm-co-MAA)/Laponite gel (Fig. 2III c) exhibited a fracture stress 3.5 times higher than organically crosslinked poly(AAm-co-MAA) gel (Fig. 2III d) due to dissipation of mechanical energy by multifunctional crosslinker Laponite. In contrast, poly(AAm-co-MAA)/Laponite/SiO₂ dual nanocomposite hydrogel, which was crosslinked by both Laponite and SiO₂, did not break down even at a strain of 100% and still maintained its configuration (only small cracks could be observed) (Fig. 2III b). The stress at 100% strain for the new hydrogel was 1.7 times higher than the fracture stress of poly(AAm-co-MAA)/Laponite gel and 11 times higher than poly(AAm-co-MAA) gel. These were observations verified that the import of inorganic hybrid crosslinking led to an enhancement in the compressive strength of the hydrogel. When free of Laponite in the preparation process, the resultant silica-based hydrogel showed high compression stress of 54.85 MPa at a strain of 100%. However, it was brittle (Fig. 2IV), and showed a tensile strain at break of 82% (for the tensile test, the hydrogels were in a size of 5.5 mm diameter \times 60 mm length). In contrast, the poly(AAm-co-MAA)/Laponite/SiO₂ dual nanocomposite hydrogel was tough with a ruptured strain of 175%, 1.1 times higher than the silica-based hydrogel, but 0.4 times lower than

the poly(AAm-co-MAA)/Laponite nanocomposite hydrogel. Moreover, it was observed a high tensile stress of 1.82 MPa for poly(AAm-co-MAA)/Laponite/SiO₂ dual nanocomposite hydrogel compared with the other controls. It suggested that the presence of nano-SiO₂ made a greater contribution on compressive strength than elongation. Direct blending of silica nanoparticles into hydrogel network could increase the strength in some degree, but compatibility problems arise in high silica content.^{20, 25, 26, 33-38} To improve the compatibility between SiO₂ nanoparticles and hydrophilic polymers, the in-situ sol-gel process was often used for the preparation of nanocomposite hydrogels utilizing organosilane as silica precursors.³⁹⁻⁴² As a consequence, in-situ preparation of SiO₂ nanoparticles in hydrogel could effectively improve the compatibility and thus enhance the mechanical strength.³⁹⁻⁴² Differently, in our present experiment, SiO₂ nanoparticles was not only connected with Laponite by covalent bonds during the in-situ sol-gel process, but also chemically connected with polymers by simultaneous free-radical polymerization.³⁹ As a result, the dual nanocomposite hydrogel exhibited satisfactory strength and toughness.

Cyclic compression-recovery test (the hydrogel with the same dimensions as in the compression test) was performed to study the fatigue resistance of hydrogel (Fig. 2V). As witnessed, the third, fourth and fifth measurements showed almost identical stress-strain behaviours to the second measurement cycle and the loading-unloading cycle curves from second to fifth showed no obvious hysteresis loops. It suggested that the dual nanocomposite structure could dissipate significant amounts of mechanical energy under large deformation and maintain their original configurations after deformation. This multiple toughening mechanism was the mainspring for the excellent fatigue resistance of the dual nanocomposite gel.

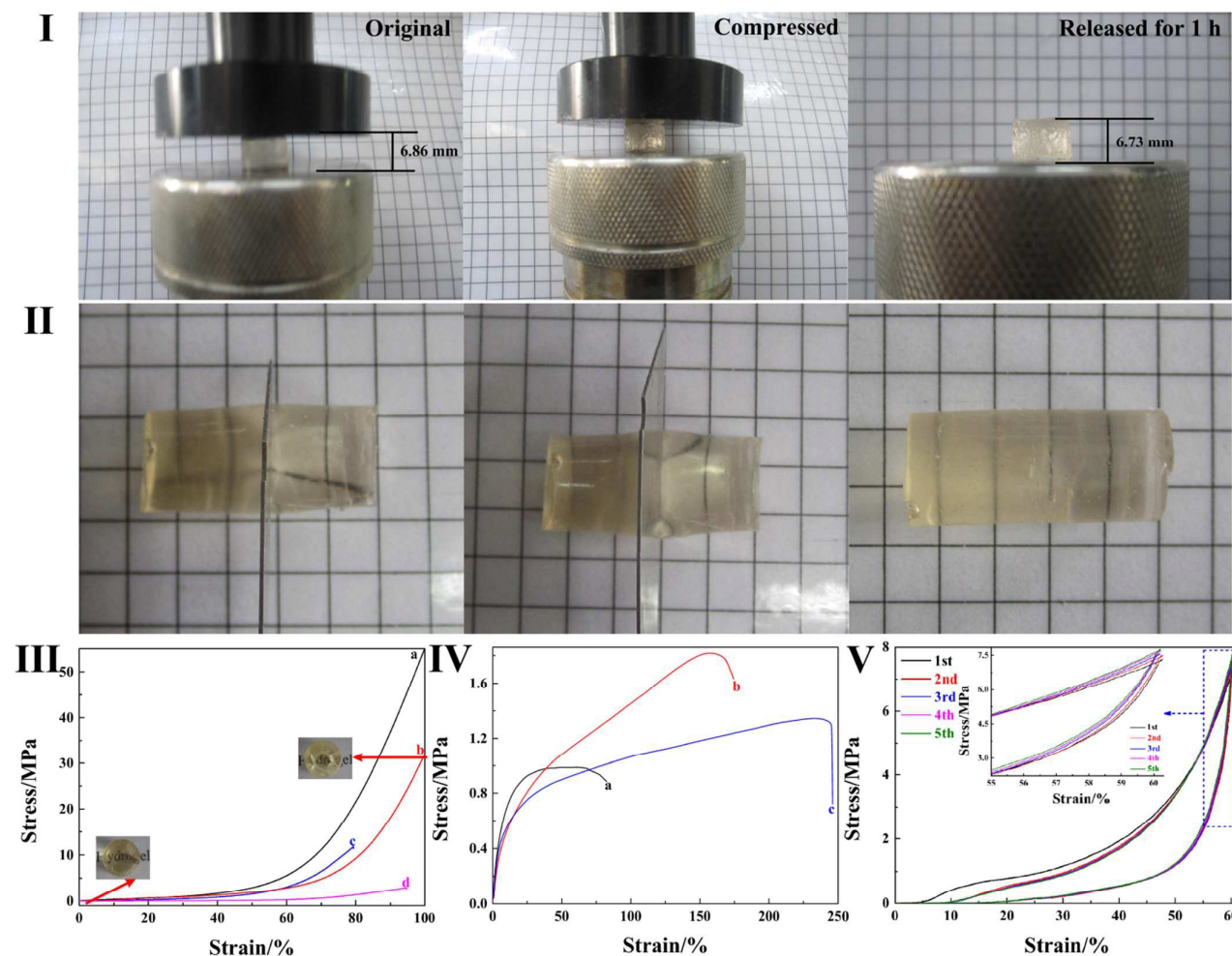


Fig. 2 I-Compressed and released state of the poly(AAm-co-MAA)/Laponite/SiO₂ dual nanocomposite hydrogel; II-The gel could not be easily cut with a knife; III-Compression stress-strain curves for: a-Poly(AAm-co-MAA)/SiO₂ nanocomposite hydrogel; b-Poly(AAm-co-MAA)/Laponite/SiO₂ dual nanocomposite hydrogel (the insert: the as-prepared gel and the gel after compressed under 100% strain); c-Poly(AAm-co-MAA)/Laponite nanocomposite hydrogel; d-Organically cross-linked poly(AAm-co-MAA) hydrogel; IV-Tensile stress-strain curves for: a-Poly(AAm-co-MAA)/SiO₂ nanocomposite hydrogel; b-Poly(AAm-co-MAA)/Laponite/SiO₂ dual nanocomposite hydrogel; c-Poly(AAm-co-MAA)/Laponite nanocomposite hydrogel; V-Cyclic stress-strain curve in compression of poly(AAm-co-MAA)/Laponite/SiO₂ dual nanocomposite hydrogel.

To our best knowledge, this is the first successful trial of synthesizing super tough hydrogel with dual nanocomposite structure. The new hydrogel innovatively integrated multiple toughening mechanisms (polymer chain fracture/high-functionality crosslinker Laponite and silica plus meso-/macro-scale composites) across multiple length scales to make it more robust under loads than existing tough hydrogels. Besides, the effect of stress concentration was greatly weakened due to improved compatibility by covalent bonds between Laponite nanoplatelets and SiO₂ nanoparticles, as well as SiO₂ and polymer matrices. The special hierarchical structure dissipated mechanical energy through inter- and intrachain complexation effectively in the hydrogel under deformation. Moreover, the architecture of the polymer chains transferred from an entangled state to disentangled state, which could absorb large amounts of energy and avoid

the breaking of the hydrogels, and offered a straightforward pathway for the production of organized nanostructures. The multiple interactions among poly(AAm-co-MAA), Laponite and SiO₂ not only maintained the physical integrity of the gel, but also enhanced the fracture resistance by bond rupture and therefore toughened the materials.

Qualitative evidence of reaction was provided by Fourier transform infrared (FTIR) spectroscopy (Fig. 3a) and ²⁹Si solid-state nuclear magnetic resonance (NMR) spectroscopy (Fig. 3b). Important absorption peaks at 1724 cm⁻¹ (-C=OOH), 1661 cm⁻¹ (-CONH-), and 1452 cm⁻¹ (-OC-N-) confirmed the presence of MAA and AAm in the gel. And the absorption bands between 800 and 1260 cm⁻¹ were described as the superimposition of various Si-O-Si and Si-OH peaks.⁴³ The absorption peaks at 1012 cm⁻¹ (Si-O stretching) and 673 cm⁻¹ (Si-O bending) in pure Laponite shifted to 1018 cm⁻¹ and 762

cm^{-1} in the dual nanocomposite hydrogel accordingly, which suggested intermolecular interactions between poly(AAm-co-MAA) or SiO_2 and Laponite. In the ^{29}Si NMR spectroscopy of the dual nanocomposite hydrogel (Fig. 3b), the different species are denoted as Q^n , T^n , and M^n , where Q, T, and M designated tetra-, tri-, and monofunctional units, respectively, and n is the number of bridging O atoms surrounding the silicon atom. Raw Laponite exhibited two characteristic resonances at -94.7 ppm and -84.8 ppm, which corresponded respectively to Q^3 trioxo coordinated framework silicon and Q^2 sites attributed to isolated silanol groups present at the silicate sheet edges.⁴⁴ The grafting was evidenced by the appearance of signals assigned to M^1 (15.0 ppm) and $T^{2,3}$ (-56.9 ppm, -66.5 ppm) silicate units derived from mono- and trialkoxysilanes, respectively, and by the decrease of the relative intensity of the Q^2 signal due to reaction with the Si-OH groups of the clay sheets.

X-ray diffraction (XRD) patterns of the hydrogel exhibited the distribution of Laponite and SiO_2 nanoparticles (Fig. 3c). A peak at $2\theta=4.88^\circ$ - 6.89° was observed in the diffraction pattern of pure Laponite, corresponding to the interplanar distance between Laponite nanosheets.⁴⁵ There was no distinct characteristic Laponite peak in the range of 2θ from 2° to 8° in the XRD pattern of the hydrogel, while at the same time we could find the characteristic diffraction peaks of SiO_2 nanoparticles at 16° .⁴⁶ These suggested that Laponite and SiO_2 nanoparticles were uniformly dispersed in the polymer gels without regular stacking. Transmission electron microscopy (TEM) analysis of the hydrogel further revealed the dispersion level of Laponite and SiO_2 (Fig. 3d). There was no obvious agglomeration of Laponite and SiO_2 , which were well-dispersed in the polymer matrix. That was the primary cause for greatly improved mechanical properties of dual nanocomposite hydrogels. From the high-resolution transmission electron microscopy (HRTEM) photographs, it observed that inorganic particles with a size of 10-20 nm were embedded in polymer matrix (Fig. 3e-g), and the characteristic elements of Laponite (Mg=13.35% and Si=29.38% in pure clay) and SiO_2 (Si) were detected by HRTEM coupled with energy-dispersive X-ray detector (HRTEM/EDS) and showed the presence of C, O, Mg and Si elements (C=1.91%, O=39.38%, Mg=1.92%, Si=56.59%), suggesting that SiO_2 and Laponite were all embedded into the polymer matrix. It further demonstrated that an organic/inorganic dual nanocomposite structure was indeed formed in the hydrogel.

In order to clarify the effect of SiO_2 and Laponite in the structure of dual nanocomposite hydrogel separately, first we prepared poly(AAm-co-MAA)/ SiO_2 hydrogel and observed core-shell structures with nano- SiO_2 as the cores and poly(AAm-co-MAA) as the shell (Fig. S2, ESI[†]). It was worth mentioning that the cores with sizes of 100-400 nm composed of several SiO_2 nanoparticles. The polymer chains connected on the surface of silica particles by covalent bonds, which presumably account for the superior compression strength of poly(AAm-co-MAA)/ SiO_2 gel.

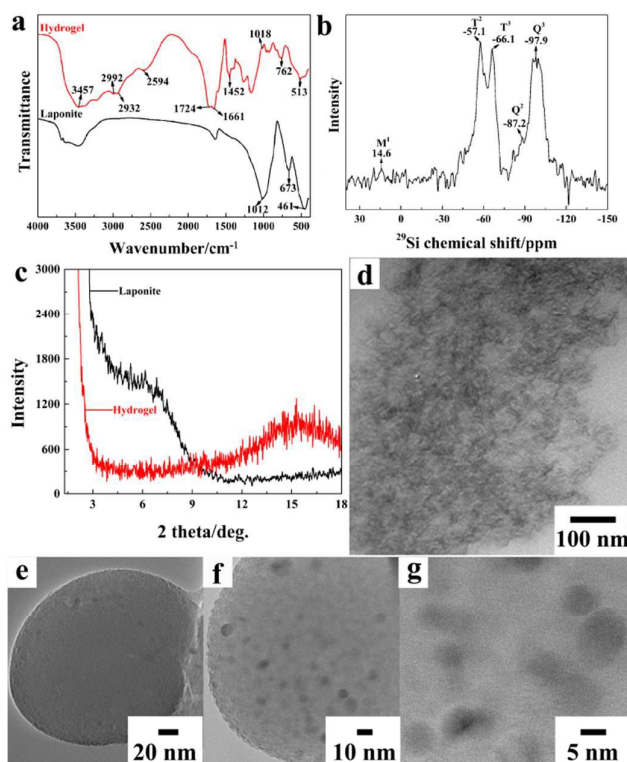


Fig. 3 FTIR (a), ^{29}Si NMR (b) spectra, XRD profiles (c), TEM (d) and HRTEM images (e-g) of poly(AAm-co-MAA)/Laponite/ SiO_2 dual nanocomposite hydrogel.

When high concentration of sodium hydroxide (NaOH) solution was used to corrode off SiO_2 , but keep clay intact in poly(AAm-co-MAA)/Laponite/ SiO_2 dual nanocomposite hydrogel, the hydrogel lost its solid-like behavior. This confirmed the crosslinking role of SiO_2 particles. TEM analysis of the NaOH-treated hydrogel exhibited several irregular pores and suggested that SiO_2 particles might exist in cluster and were firmly attached to each other (Fig. S3, ESI[†]). This was confirmed by HRTEM results (Fig. 3e-g). To figure out the distribution state of Laponite and SiO_2 in detail, hydrofluoric acid (HF) was utilized to decompose off Laponite and SiO_2 (Fig. 4a-b). When inorganic particles were rotted in a short time (24 h) (Fig. 4a), and eye-like constructions could be found due to the different removal degree of Laponite and SiO_2 from the hydrogel. If the inorganic particles were corroded away after a longer time (48 h) (Fig. 4b), hydrogel framework would totally be destroyed, and numerous irregular pores were observed. The multiple pores testified the diverse distribution modes of Laponite and SiO_2 in the polymer matrix. The distinct existence of SiO_2 and Laponite nanoparticles made it more efficient to act as dual crosslinking agents during polymerization and building blocks for creating organic-inorganic nanocomposites. The resultant hydrogel with dual nanocomposite construction possessed high compressive strength. According to the results above, it can be concluded that the special distribution forms and chemical interactions of SiO_2 and Laponite are the critical factor to obtain tough hydrogel.

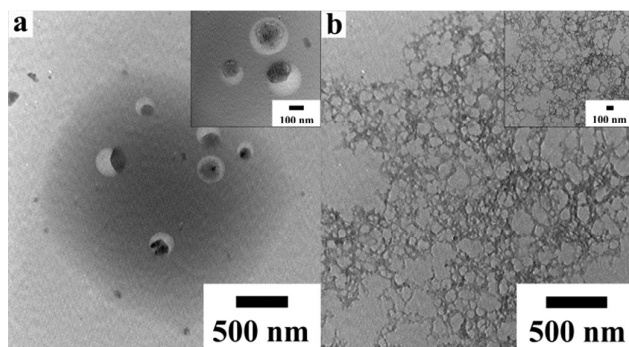


Fig. 4 TEM images of poly(AAm-co-MAA)/Laponite/SiO₂ dual nanocomposite hydrogel treated by HF (20 wt%) for 24 h (a) and 48 h (b), respectively.

In summary, we integrated dual nanocomposite reinforcement to develop a novel hydrogel poly(AAm-co-MAA)/Laponite/SiO₂ with an unprecedented compressive strength of 32.00 MPa without rupture even at 100% strain. Covalent bonds existed between SiO₂ and Laponite, as well as between polymers and SiO₂, which strengthened the compatibility of inorganic fillers with polymer matrices. Furthermore, inorganic hybrid crosslinking and hierarchy structure of SiO₂ and Laponite improved the endurance of loads. Due to the strengthening mechanism of dual nanocomposite, the hydrogels exhibited extraordinary fatigue resistant properties during five compression cycles. With high strength and toughness, the hydrogel might be used as a potential candidate in bioengineering, artificial soft tissues and drug delivery systems. In addition, the multi-strengthening mechanism of particular dual nanocomposite is developed to effectively dissipate energy and maintain elasticity of hydrogels. This new mechanism can provide a promising strategy for the design of future tough hydrogels with extraordinary properties.

Acknowledgments

The work was supported by the NSFC-Xinjiang joint fund for local outstanding youth (No.U1403392), the International Science and Technology Cooperation Project (No.20146008), and the Excellent Doctor Innovation Program of Xinjiang University (No.XJUBSCX-2014011).

Notes and references

- J. R. Xavier, T. Thakur, P. Desai, M. K. Jaiswal, N. Sears, E. Cosgriff-Hernandez, R. Kaunas and A. K. Gaharwar, *ACS Nano*, 2015, **9**, 3109-3118.
- G. D. Nicodemus and S. J. Bryant, *Tissue Eng. Part B*, 2008, **14**, 149-165.
- Z. Li, Y. Su, B. Xie, H. Wang, T. Wen, C. He, H. Shen, D. Wu and D. Wang, *J. Mater. Chem. B*, 2013, **1**, 1755-1764.
- K. Y. Lee and D. J. Mooney, *Chem. Rev.*, 2001, **101**, 1869-1880.
- T. R. Hoare and D. S. Kohane, *Polymer*, 2008, **49**, 1993-2007.

- M. A. Haque, T. Kurokawa and J. P. Gong, *Polymer*, 2012, **53**, 1805-1822.
- Y. Osada, H. Okuzaki and H. Hori, *Nature*, 1992, **355**, 242-244.
- N. A. Peppas, J. Z. Hilt, A. Khademhosseini and R. Langer, *Adv. Mater.*, 2006, **18**, 1345-1360.
- A. P. Nowak, V. Breedveld, L. Pakstis, B. Ozbas, D. J. Pine, D. Pochan and T. J. Deming, *Nature*, 2002, **417**, 424-428.
- P. Calvert, *Adv. Mater.*, 2009, **21**, 743-756.
- J. Kim, J. A. Hanna, M. Byun, C. D. Santangelo and R. C. Hayward, *Science*, 2012, **335**, 1201-1205.
- Y. Okumura and K. Ito, *Adv. Mater.*, 2001, **13**, 485-487.
- J. P. Gong, Y. Katsuyama, T. Kurokawa and Y. Osada, *Adv. Mater.*, 2003, **15**, 1155-1158.
- T. Huang, H. Xu, K. Jiao, L. Zhu, H. R. Brown and H. Wang, *Adv. Mater.*, 2007, **19**, 1622-1626.
- T. Sakai, T. Matsunaga, Y. Yamamoto, C. Ito, R. Yoshida, S. Suzuki, N. Sasaki, M. Shibayama and U.-i. Chung, *Macromolecules*, 2008, **41**, 5379-5384.
- D. C. Tuncaboylu, M. Sari, W. Oppermann and O. Okay, *Macromolecules*, 2011, **44**, 4997-5005.
- K. J. Henderson, T. C. Zhou, K. J. Otim and K. R. Shull, *Macromolecules*, 2010, **43**, 6193-6201.
- Y. Zhang, Y. Li and W. Liu, *Adv. Funct. Mater.*, 2015, **25**, 471-480.
- K. Haraguchi and T. Takehisa, *Adv. Mater.*, 2002, **14**, 1120.
- S. Rose, A. Marcellan, T. Narita, F. Boué, F. Cousin and D. Hourdet, *Soft Matter*, 2015, **11**, 5905-5917.
- X. Nie, A. Adalati, J. Du, H. Liu, S. Xu and J. Wang, *Appl. Clay Sci.*, 2014, **97**, 132-137.
- A. Shiotani, T. Mori, T. Niidome, Y. Niidome and Y. Katayama, *Langmuir*, 2007, **23**, 4012-4018.
- R. Liu, S. Liang, X.-Z. Tang, D. Yan, X. Li and Z.-Z. Yu, *J. Mater. Chem.*, 2012, **22**, 14160-14167.
- B. Xu, H. Li, Y. Wang, G. Zhang and Q. Zhang, *RSC Adv.*, 2013, **3**, 7233-7236.
- J. Yang, C.-R. Han, X.-M. Zhang, F. Xu and R.-C. Sun, *Macromolecules*, 2014, **47**, 4077-4086.
- J. Yang, C.-R. Han, J.-F. Duan, F. Xu and R.-C. Sun, *J. Phys. Chem. C*, 2013, **117**, 8223-8230.
- X. Zhao, *Soft Matter*, 2014, **10**, 672-687.
- Q. Chen, D. Wei, H. Chen, L. Zhu, C. Jiao, G. Liu, L. Huang, J. Yang, L. Wang and J. Zheng, *Macromolecules*, 2015, **48**, 8003-8010.
- Y. Tanaka, J. P. Gong and Y. Osada, *Prog. Polym. Sci.*, 2005, **30**, 1-9.
- S. Naficy, H. R. Brown, J. M. Razal, G. M. Spinks and P. G. Whitten, *Aust. J. Chem.*, 2011, **64**, 1007-1025.
- Y. Abe, Y. Honda and T. Gunji, *Appl. Organometal. Chem.*, 1998, **12**, 749-753.
- J. Du, R. Wu, H. Liu, X. Nie, H. Li, S. Xu and J. Wang, *Polym. Composite.*, 2015, **36**, 538-544.
- A. K. Gaharwar, C. Rivera, C.-J. Wu, B. K. Chan and G. Schmidt, *Mat. Sci. Eng. C-Mater.*, 2013, **33**, 1800-1807.
- W.-C. Lin, W. Fan, A. Marcellan, D. Hourdet and C. Creton, *Macromolecules*, 2010, **43**, 2554-2563.
- S. v. Rose, A. Dizeux, T. Narita, D. Hourdet and A. Marcellan, *Macromolecules*, 2013, **46**, 4095-4104.

36. M. Takafuji, S.-y. Yamada and H. Ihara, *Chem. Commun.*, 2011, **47**, 1024-1026.
37. M. A. Alam, M. Takafuji and H. Ihara, *J. Colloid Interf. Sci.*, 2013, **405**, 109-117.
38. N. Miyamoto, K. Shimasaki, K. Yamamoto, M. Shintate, Y. Kamachi, B. P. Bastakoti, N. Suzuki, R. Motokawa and Y. Yamauchi, *Chem.-Eur. J.*, 2014, **20**, 14955-14958.
39. X. Shi, S. Xu, J. Lin, S. Feng and J. Wang, *Mater. Lett.*, 2009, **63**, 527-529.
40. Y. L. Li, N. Ouyang, A. R. Ke and S. B. Lin, *J. Appl. Polym. Sci.*, 2013, **128**, 761-766.
41. Y. Chen, W. Xu and G. Zeng, *J. Mater. Sci.*, 2014, **49**, 7360-7370.
42. N. Sahiner, *Colloid Polym. Sci.*, 2007, **285**, 413-421.
43. A. Beganskienė, V. Sirutkaitis, M. Kurtinaitienė, R. Juškėnas and A. Kareiva, *Mater. Sci. (Medžg.)*, 2004, **10**, 287-290.
44. N. N. Herrera, J.-M. Letoffe, J.-L. Putaux, L. David and E. Bourgeat-Lami, *Langmuir*, 2004, **20**, 1564-1571.
45. Q. Zhang, X. Li, Y. Zhao and L. Chen, *Appl. Clay Sci.*, 2009, **46**, 346-350.
46. L. P. Singh, S. K. Agarwal, S. K. Bhattacharyya, U. Sharma and S. Ahalawat, *Nanomater. Nanotechno.*, 2011, **1**, 44-51.



RSC Matter

COMMUNICATION

Tough dual nanocomposite hydrogels with inorganic hybrid crosslinking

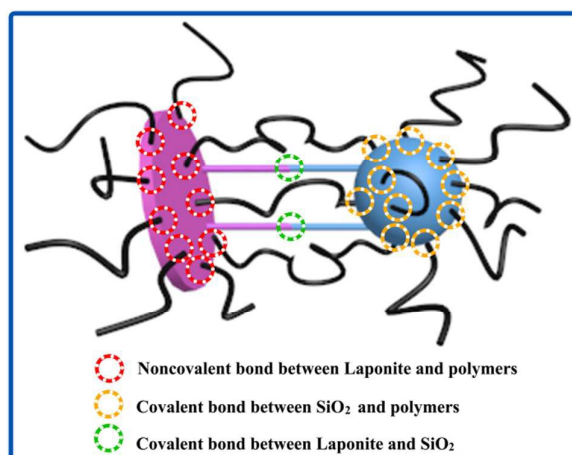
Received 00th January 20xx,
Accepted 00th January 20xx

Juan Du, Shimei Xu*, Shun Feng, Lina Yu, Jide Wang*, and Yumei Liu

DOI: 10.1039/x0xx00000x

www.rsc.org/

Graphical Abstract



Due to the multi-strengthening mechanism of dual nanocomposite, a super tough and strong hydrogel with inorganic hybrid crosslinking was fabricated.

Key Laboratory of Oil and Gas Fine Chemicals, Ministry of Education and Xinjiang Uyghur Autonomous Region, College of Chemistry and Chemical Engineering, Xinjiang University, Urumqi, Xinjiang 830046, People's Republic of China; Fax: + 86 991 8581018; Tel: + 86 991 8583972; E-mail: xushmei@hotmail.com, awangjd@xju.edu.cn

† Electronic Supplementary Information (ESI) available: Experimental procedures; Retention time dependence of transparency and viscosity; TEM images of poly(AAm-co-MAA)/SiO₂ nanocomposite hydrogel; TEM images of poly(AAm-co-MAA)/Laponite/SiO₂ dual nanocomposite hydrogel treated by NaOH. See DOI: 10.1039/x0xx00000x